Preparation of $PbZrO_3/ASO_4$ Composites (A = Ca, Sr, Ba) and $PbZrO_3$ by Metathetic Reactions in the Solid State: Metathetic Exchange of Divalent Species

Monalisa Panda,† Ram Seshadri,* and J. Gopalakrishnan

Solid State and Structural Chemistry Unit, Indian Institute of Science, Bangalore 560 012, India

Received October 29, 2002

Metathetic solid-state reactions of alkaline earth perovskite zirconates ($AZrO_3$, A = Ca, Sr, Ba) and lead sulfate ($PbSO_4$) result in the relatively quick formation of perovskite $PbZrO_3$ and the corresponding alkaline earth sulfate ASO_4 at temperatures as low as 1023 K. The product can be described as a composite dispersion of small (<300 nm) particles of $PbZrO_3$ on larger crystals of the alkaline earth sulfates. The solid-state reaction at 973 K between ZrO_2, $PbSO_4$, and K_2CO_3 followed by washing in water to remove K_2SO_4 provides a quick route to submicron (<1 μm) $PbZrO_3$ powders starting from inexpensive precursors. In all the reactions, we believe the driving force to be the high enthalpy of formation of ASO_4 or K_2SO_4. The reactions presented here provide proof of concept for the preparation of a number of important polar lead-based perovskite phases under relatively mild conditions: (i) as composites, (ii) as small particles, and (iii) possibly as porous monoliths.

Introduction

Apropos the synthesis of inorganic compounds and its relevance to materials science and engineering, it is useful to recognize that there are two classes of inorganic materials synthesis: one in which new compounds ensue, perhaps to serve a specific purpose, and the other in which known compounds are obtained through new routes or in new forms.[1] An illustration of the latter is preparation of the mineral magnetite in nanoparticulate form. Whereas the compound (meaning the crystal structure) would by no means be new, in the process of making it as small particles, the material obtained could be regarded as novel.

One of our recent avenues of interest has been in attempting to pattern materials at large (micrometer) length scales. We use the term *pattern* as distinct from *structure* (the local coordinations of atoms) to indicate the manner in which crystallites of the material are assembled in the polycrystalline monolith. Within this rubric, we include textured or porous materials. Inspired by ordered micrometer-sized pores in certain biogenic calcites, notably the skeletal plates of sea-urchins,[2] we have been pursuing the preparation of macroporous materials using biogenic templates[3] as well as template-free routes. The segregation of certain oxide phases, formed upon decomposing single-source precursors[4] or through combustion synthesis,[5] can yield monoliths from which one of the oxide phases can be selectively leached out resulting in macroporosity, with connected albeit disordered pores, a few micrometers in diameter. In the course of such preparations, we been made aware of the importance of preparing piezoelectric compounds in porous form for applications as actuator materials.[6] When made porous, the so-called hydrophone figure of merit of $PbZrO_3$ is expected to be greatly increased because of the larger compliance associated with porosity.

To this end, we have been inspired by the work of Epple and Herzberg[7] in their preparation of porous polyglycolide, in seeking metathetic reactions of the kind

$$AB + CD \rightarrow AC + BD$$

where AC might be the compound that we wish to prepare in porous form, and BD might be water soluble and hence easily leached out of a monolith containing the products.

Metathetic reactions have been used in the preparation of known materials in novel and rapid ways[8] as well as for the stabilization of novel metastable phases.[9] Their utility in the production of patterned inorganic materials is, however, not often encountered. Two examples that we have come across in the literature are the preparation of porous silicon imido nitrides from the

* To whom correspondence should be addressed at current location: Materials Department, University of California Santa Barbara, Santa Barbara, CA 93106-5050. Fax: (805) 893 8797. E-mail: seshadri@mrl.ucsb.edu.

† Present address: Institut für Anorganische und Angewandte Chemie, Universität Hamburg, Martin Luther King Platz 6, 20146 Hamburg, Germany.

(1) Rao, C. N. R.; Gopalakrishnan, J. *New Directions in Solid State Chemistry*, 2nd ed.; Cambridge University Press: Cambridge, 1997.

(2) Donnay, G.; Pawson, D. L. *Science* **1969**, *166*, 1147; Nissen, H.-U. *Science* **1969**, *166*, 1150.

(3) Meldrum, F. C.; Seshadri, R. *J. Chem. Soc., Chem. Commun.* **2000**, *29*; Seshadri, R.; Meldrum, F. C. *Adv. Mater.* **2000**, *12*, 1149.

(4) Rajamathi, M.; Thimmaiah, S.; Morgan, P. E. D.; Seshadri, R. *J. Mater. Chem.* **2001**, *11*, 2489.

(5) Panda, M.; Rajamathi, M.; Seshadri, R. *Chem. Mater.* **2002**, *14*, 4762.

(6) Trolier-McKinstry, S.; Newnham, R. E. *MRS Bull.* **1994**, *18*, 27.

(7) Epple, M.; Herzberg, O. *J. Mater. Chem.* **1997**, *7*, 1037.

(8) Bonneau, R. P.; Jarvis, R. F., Jr.; Kaner, R. B. *Nature* **1991**, *349*, 510; Wiley, J. B.; Kaner, R. B. *Science* **1992**, *255*, 1093.

10.1021/cm021065z CCC: $25.00
Published on Web 03/11/2003

metathetic reaction of $SiCl_4$ with NH_3,[10] and of TiO_2 nanocrystals from the reaction $Ti(OR)_4 + TiX_4 \rightarrow 2TiO_2 + 4RX$ performed in trioctyl phosphine oxide as solvent.[11] A notable point in the work presented here arises from our having achieved metathesis between multivalent species in the solid state. Most metathetic reactions involve the diffusion and reaction of monovalent species, the elimination of alkali halides being an example. We know of one previous example where the sulfate ion is involved in solid-state metathesis but there too, in conjunction with monovalent Li^+.[12] Likewise, while nitrides[13] and borides[14] which are multivalent species have been prepared using metathesis, in these reactions too are halides of alkaline earths formed.

The reaction of zircon with dolomite has been studied in situ, using powder neutron thermodiffractometry, by Rodríguez et al.[15] The reaction gives $CaZrO_3$ as a product, and is closer to a true example of multivalent metathesis. Suzuki et al.[16] have subjected mixtures of dolomite and ZrO_2 to reactive hot-pressing, and thereby prepared $MgO/CaZrO_3$ composites.

Here we report the preparation of $PbZrO_3$ in composites with other inorganic materials, as well as attempts to prepare it in porous form using simple metathetic routes. We have not succeeded in the second goal of making porous materials, but in trying to do so, have devised a method for making small, crystalline particles of $PbZrO_3$ at relatively low temperatures. Making Pb compounds at reduced temperatures is always an issue because of the volatility and toxicity of Pb oxides.

Routes to preparing fine powders of $PbZrO_3$ usually involve high-energy precursors (nitrates, chlorides, etc.) and recent reports include the following: by Camarago et al.[17] starting from nitrates heated to 973 K, by Choy and Han[18] starting from citrates heated to between 873 and 1073 K, and by Choy et al.[19] from oxalates heated between 873 and 1073 K. A systematic study of the size-dependent antiferroelectric transition has been performed by Chattopadhyay et al.[20] on samples of small-particulate $PbZrO_3$ prepared by heating precipitated hydroxides in a controlled manner above 923 K. In none of these reports have the $PbZrO_3$ samples been subjected to careful structural analysis as we have done in the present work. Consequently, making comparisons of the sample quality of the particles obtained from these different methods has not been possible.

Experimental Section

The starting perovskite materials $AZrO_3$ were prepared from 0.02 mol alkaline earth carbonates ($CaCO_3$ 2.00 g; $SrCO_3$ 2.95 g; or $BaCO_3$ 3.94 g) and 0.02 mol ZrO_2 (2.46 g). These were ground intimately, pelletized, and fired at 1223 K in air for 24 h. The pellets were then removed, ground finely, pelletized again, and fired in air at 1273 K for 24 h.

The preparation of $PbZrO_3/ASO_4$ composites involved the reaction of 0.015 mol alkaline earth zirconate ($CaZrO_3$ 0.26 g; $SrZrO_3$ 0.31 g; or $BaZrO_3$ 0.41 g) with 0.015 mol $PbSO_4$ (0.45 g). The powders were carefully ground together and pressed into pellets 10 mm in diameter and 2−3 mm high. They were heat-treated in air at 1023 K for 12 h. The heating of lead oxides in open tube furnaces is best performed in a fume hood because of the high volatility of PbO at elevated temperatures. Milder conditions (shorter times, lower temperatures) were not attempted. Harsher conditions (longer times, higher temperatures) resulted in ZrO_2 reflections appearing in the powder X-ray diffraction (XRD) profiles, perhaps due to evaporative loss of PbO.

Pure $PbZrO_3$ powders were prepared in the following way. A mixture of 0.002-mol each of $PbSO_4$ (0.60 g), ZrO_2 (0.24 g), and K_2CO_3 (0.28 g) was ground intimately and pelletized as above. The pellets were heat treated in air at 973 K for 12 h. To remove K_2SO_4 from the product, the pellet was placed in a beaker of deionized water for 24 h with periodic replacement of the water.

Samples were studied by powder XRD using a Siemens D5005 diffractometer with the following conditions: $\theta-2\theta$ geometry, Cu Kα radiation, 2° 2θ/min. scan rate, data rebinned into 0.02° 2θ steps. For scanning electron microscopy, samples were mounted using double-sided conducting carbon tape on brass stubs and gold-coated to avoid charging. A JEOL JSM 5600 LV microscope operating in the high-vacuum mode was used. Both secondary electron (SE) and backscattered electron imaging modes were employed. The instrument was equipped with a Link/ISIS system from Oxford Instruments for energy-dispersive X-ray (EDX) analysis.

Results

Rietveld refinements using the XND Rietveld code[21] of the starting $AZrO_3$ (A = Ca, Sr, Ba) materials prepared by us confirmed their phase purity. Starting structural models were the reported orthorhombic *Pnma* ($CaZrO_3$) or cubic $Pm\bar{3}m$ ($SrZrO_3$, $BaZrO_3$) structures.[22] No extra reflections were observed in the patterns, except for very small amounts of unreacted ZrO_2 manifesting as a peak around 28° 2θ in the $SrZrO_3$ and $BaZrO_3$ patterns. The agreement factors from the refinements were, respectively, $R_{Bragg} = 6.4\%$, 2.8%, and 3.6% for the Ca, Sr, and Ba zirconates.

The first class of reactions that we attempted were the following:

$$AZrO_3 + PbSO_4 \rightarrow ASO_4 + PbZrO_3;\ A = Ca, Sr, Ba \quad (1)$$

The next three figures display results of Rietveld analysis of the powder XRD profiles of the products of the reaction of $PbSO_4$ with $CaZrO_3$ (Figure 1), $SrZrO_3$

(9) Gopalakrishnan, J.; Sivakumar, T.; Ramesha, K.; Thangadurai, V.; Subbanna, G. N. *J. Am. Chem. Soc.* **2000**, *122*, 6237; Sivakumar, T.; Seshadri, R.; Gopalakrishnan, J. *J. Am. Chem. Soc.* **2001**, *123*, 11496; Kodenkandath, T. A.; Lalena, J. N.; Zhou, W. L.; Carpenter, E. E.; Sangregorio, C.; Falster, A. U.; Simmons, W. B., Jr.; O'Connor, C. J.; Wiley, J. B. *J. Am. Chem. Soc.* **1999**, *121*, 10743. For a recent review, see Schaak, R. E.; Mallouk, T. E. *Chem. Mater.* **2002**, *14*, 1455.

(10) Kaskel, S.; Farrusseng, D.; Schlichte, K. *J. Chem. Soc., Chem. Commun.* **2000**, 2481.

(11) Trentler, T. J.; Denler, T. E.; Bertone, J. F.; Agrawal, A.; Colvin, V. L. *J. Am. Chem. Soc.* **1999**, *121*, 1613.

(12) Hedden, D. B.; Torardi, C. C.; Zegarski, W. *J. Solid State Chem.* **1995**, *118*, 419.

(13) Hector, A. L.; Parkin, I. P. *Chem. Mater.* **1995**, *7*, 1728.

(14) Rao, L.; Gillan, E. G.; Kaner, R. B. *J. Mater. Res.* **1996**, *10*, 353.

(15) Rodríguez, J. L.; De Aza, A. H.; Pena, P.; Campo, J.; Convert, P.; Turrullas, X. *J. Solid State Chem.* **2002**, *166*, 426.

(16) Suzuki, Y.; Morgan, P. E. D.; Ohji, T. *Mater. Sci. Eng. A* **2001**, *304*, 780.

(17) Camarago, E. R.; Popa, M.; Frantti, J.; Kakihana, M. *Chem. Mater.* **2001**, *13*, 3943.

(18) Choy, J.-H.; Han, Y.-S. *J. Mater. Chem.* **1997**, *7*, 1815.

(19) Choy, J.-H.; Han, Y.-S.; Kim, S.-J. *J. Mater. Chem.* **1997**, *7*, 1807.

(20) Chattopadhyay, S.; Ayyub, P.; Palkar, V. R.; Gurjar, A. V.; Wankar, R. M.; Multani, M. *J. Phys.: Condens. Matter* **1997**, *9*, 8135.

(21) Bérar, J.-F.; Garnier, P. NIST Special Publication **1992**, *846*, 212; Freely available from the CCP14 website at http://www.ccp14.ac.uk.

(22) $CaZrO_3$: Koopmanns, H. J. A.; van de Velde, C. M. H.; Gellings, P. J. *Acta Crystallogr. C* **1983**, *39*, 1323. $SrZrO_3$: Hoffmann, A. *Naturwiss.* **1933**, *21*, 676. $BaZrO_3$: ICDD card 6-399.

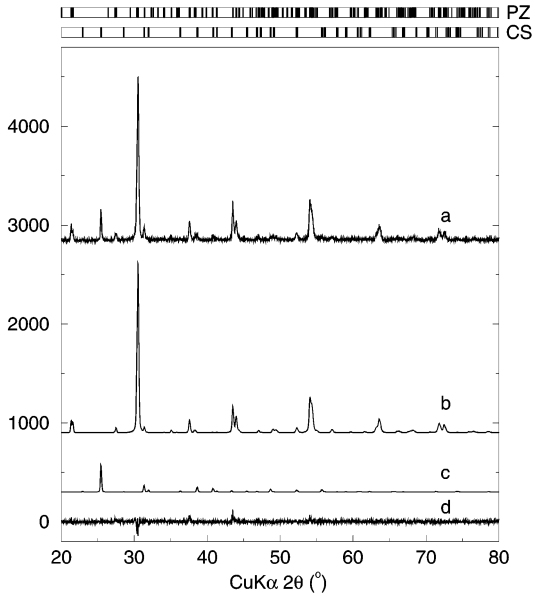

Figure 1. X-ray powder pattern of the $PbZrO_3/CaSO_4$ composite showing data (a), the Rietveld fit to the $PbZrO_3$ component (b), the Rietveld fit to the $CaSO_4$ component (c), and the difference profile (d). Vertical lines at the top of the figure indicate expected peak positions for $PbZrO_3$ (PZ) and $CaSO_4$ (CS).

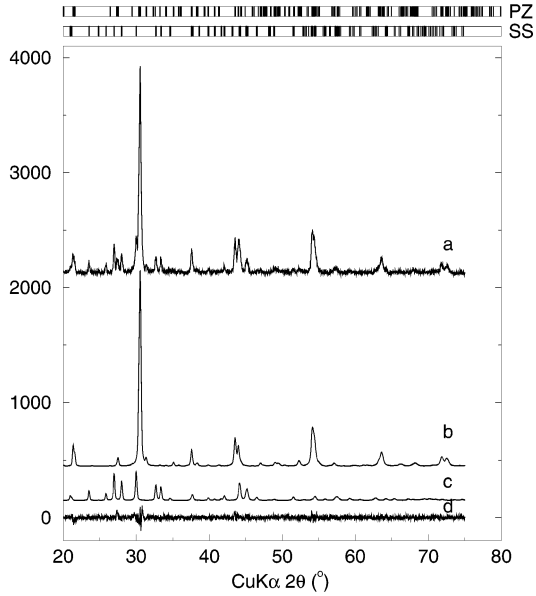

Figure 2. X-ray powder pattern of the $PbZrO_3/SrSO_4$ composite showing data (a), the Rietveld fit to the $PbZrO_3$ component (b), the Rietveld fit to the $SrSO_4$ component (c), and the difference profile (d). Vertical lines at the top of the figure indicate expected peak positions for $PbZrO_3$ (PZ) and $SrSO_4$ (SS).

(Figure 2), and $BaZrO_3$ (Figure 3). Rietveld refinements made use of two-phase structural models, where one of the phases was the orthorhombic (*Pbam*) antiferroelectric structure of $PbZrO_3$[23] while the other phase was orthorhombic $CaSO_4$ anhydrite,[24] orthorhombic SrSO4 celestite,[24] or orthorhombic $BaSO_4$ barite.[25] Refinements

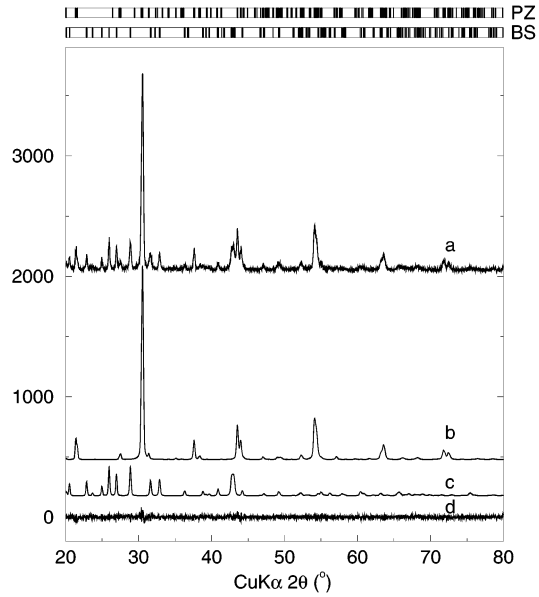

Figure 3. X-ray powder pattern of the $PbZrO_3/BaSO_4$ composite showing data (a), the Rietveld fit to the $PbZrO_3$ component (b), the Rietveld fit to the $BaSO_4$ component (c), and the difference profile (d). Vertical lines at the top of the figure indicate expected peak positions for $PbZrO_3$ (PZ) and $BaSO_4$ (BS).

Table 1. Results of the Rietveld Refinements of Two-phase $PbZrO_3/ASO_4$ (A = Ca, Sr, Ba)

system	overall R_{Bragg}	$PbZrO_3$:ASO_4	$PbZrO_3$ cell volume (Å^3)[a]	9-coordinate radius (Å)[b]
Ca	6.4%	53:47	568.6(2)	1.18
Sr	2.8%	44:56	568.4(4)	1.31
Ba	3.6%	53:47	570.0(3)	1.47

[a] To be compared with the 297 K value of 570.8(4) Å^3 obtained by Glazer and co-workers.[23] [b] To be compared with the radius of 9-coordinate Pb^{2+} which is 1.35 Å.

confirmed that these were the only phases. Rietveld scale factors permitted us to obtain quantitative estimates of mole ratios of the different phases in the product powders. The formula used for the purpose was[26]

$$W_j = (S_j Z_j M_j V_j)/\Sigma_i (S_i Z_i M_i V_i)$$

where W_j is the mole weight of component j, S is the scale factor obtained from the Rietveld refinement, Z is the number of formula units in the unit cell, M is the formula weight, and V is the unit cell volume. The summation i is over all (two) phases. Because of problems in estimating particle size, we did not employ corrections due to microabsorption as suggested by Brindley.[26] Unit cell volumes of the $PbZrO_3$ phases obtained from the three reactions were calculated using the formula provided by Giacovazzo.[27] Table 1 lists the agreement factors (R_{Bragg}) and the quantitative estimates from the two phase refinements. We find that within a 5% error (acceptable in the absence of the Brindley correction[28]), the ratios of the two phases correspond to complete metathesis between the starting

(23) Glazer, A. M.; Roleder, K.; Dec, J. *Acta Crystallogr. B* **1993**, *49*, 846.
(24) Hawthorne, F. C.; Ferguson, R. B. *Canad. Mineral.* **1975**, *13*, 289.
(25) Hill, R. J. *Canad. Mineral.* **1977**, *15*, 522.
(26) Brindley, G. W. *Philos. Mag.* **1945**, *36*, 347.
(27) Giacovazzo, C. (ed.). *Fundamentals of Crystallography*, IUCr−Oxford: New York, 1992; pp 122−123.
(28) Taylor, J. C.; Matulis, C. E. *J. Appl. Crystallogr.* **1991**, *24*, 14.

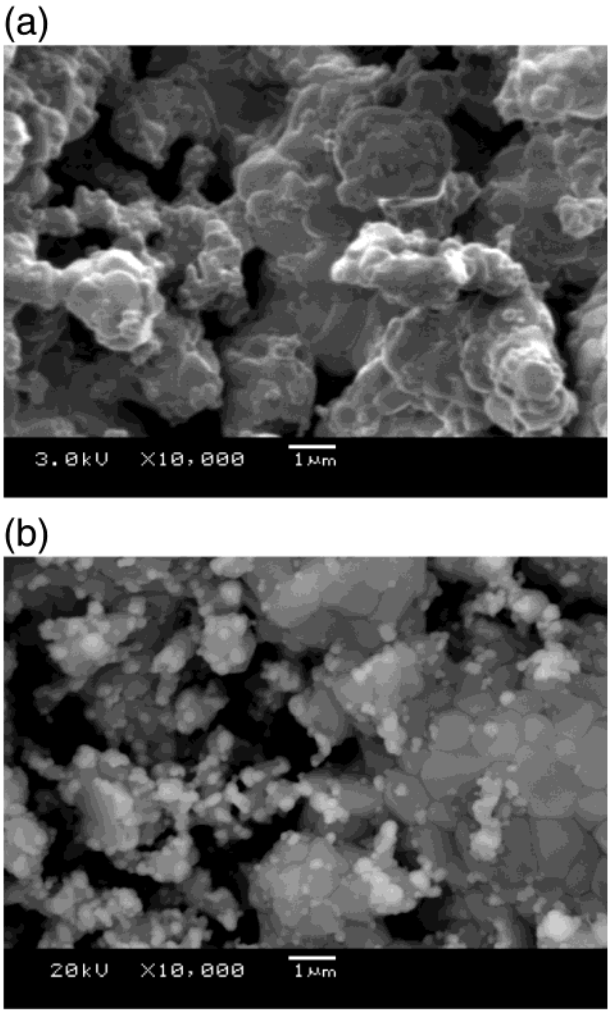

Figure 4. (a) Secondary electron (SE) SEM image of the $PbZrO_3/BaSO_4$ composite. The smaller crystals are the heavier (in terms of average atomic number) $PbZrO_3$ as testified by the backscattered electron SEM image (b).

materials. One of our concerns was that in the product $PbZrO_3$ there might be some A ion substitution in the Pb site. To address this, we calculated the unit cell volumes of the $PbZrO_3$ phases obtained from the three reactions using the formula provided by Giacovazzo.[27] Table 1 also lists the unit cell volumes and the Shannon−Prewitt radii[29] of 9-coordinate A^{2+} (A = Ca, Sr, Ba). The smaller cell volumes of the $PbZrO_3$ phases obtained from the metathesis with Ca and Sr zirconates does indeed suggest some small substitution. There is no evidence that the larger Ba^{2+} substitutes for Pb^{2+} in $PbZrO_3$, however.

Figure 4(a) displays the SE-SEM image of the $PbZrO_3/BaSO_4$ composite prepared by metathesis. Spot EDX analysis suggested that the larger crystals are $BaSO_4$ and the smaller ones are $PbZrO_3$. This is supported by the image in panel (b) which was acquired in the backscattered electron imaging mode. In this mode the heavier (meaning higher average atomic number) particles appear bright, while the lighter ones appear dark. We observe that the smaller particles in this image are indeed brighter, corresponding to $PbZrO_3$. The particles

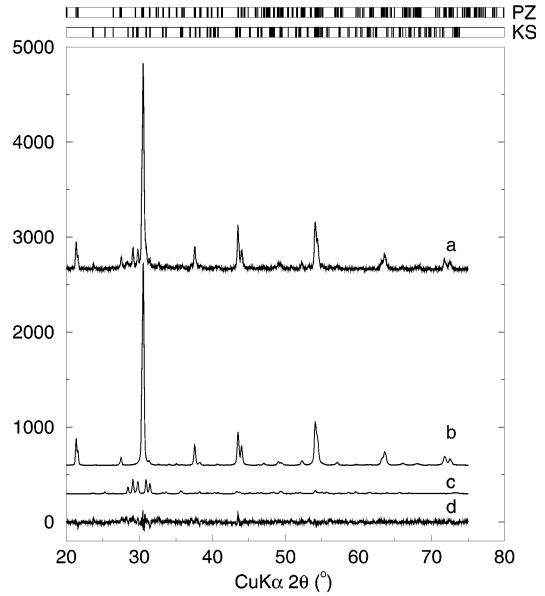

Figure 5. X-ray powder pattern of the $PbZrO_3/K_2SO_4$ composite showing data (a), the Rietveld fit to the $PbZrO_3$ component (b), the Rietveld fit to the K_2SO_4 component (c), and the difference profile (d). Vertical lines at the top of the figure indicate expected peak positions for $PbZrO_3$ (PZ) and K_2SO_4 (KS).

are typically sub-1-μm, of the order of 300 nm. The larger well-sintered particles are darker and must then correspond to $BaSO_4$.

Similarly SEM images of the $PbZrO_3/CaSO_4$ composite and the $PbZrO_3/SrSO_4$ composite revealed large, well-sintered particles of $SrSO_4$, interspersed with smaller particles of $PbZrO_3$. In all the systems, we obtain a far greater degree of intimacy in the mixing of the two phases than would be achieved by physical dispersion.

The second class of reaction that we attempted was the following:

$$PbSO_4 + ZrO_2 + K_2CO_3 \rightarrow K_2SO_4 + PbZrO_3 + CO_2\uparrow \quad (2)$$

Figure 5 displays the two-phase Rietveld fit to the powder XRD pattern obtained at the end of the reaction. The fit testifies to the product comprising only of $PbZrO_3$ and tetragonal β-K_2SO_4.[30] An overall agreement factor (R_{Bragg}) of 10.1% was obtained for this fit. Quantitative phase analysis suggested a $PbZrO_3$:K_2SO_4 mol ratio of 61:39. This is significantly different from the expected 50:50 ratio. We believe the source of this discrepancy to be the inevitable leaching of some of the K_2SO_4 crystallites by atmospheric moisture. The refined cell volume of the $PbZrO_3$ formed in this reaction, 568.6(5) Å^3, indicated that there was no substitution on the Pb site. Completely leaching out the K_2SO_4 by soaking in water does indeed result in nearly pure, monophasic $PbZrO_3$, the powder XRD pattern of which is displayed in Figure 6. The Rietveld fit (R_{Bragg} = 11.9%) indicates only one peak just below 25° in 2θ that is not fitted. The refined unit cell volume was found to be 569.2(3) Å^3, very close to the expected value of 570.8 Å^3.

(29) Shannon, R. D.; Prewitt, C. T. *Acta Crystallogr.* **1969**, *B25*, 925; Shannon, R. D. *Acta Crystallogr.* **1976**, *A32*, 751.

(30) Robinson, M. T. *J. Phys. Chem.* **1958**, *62*, 925.

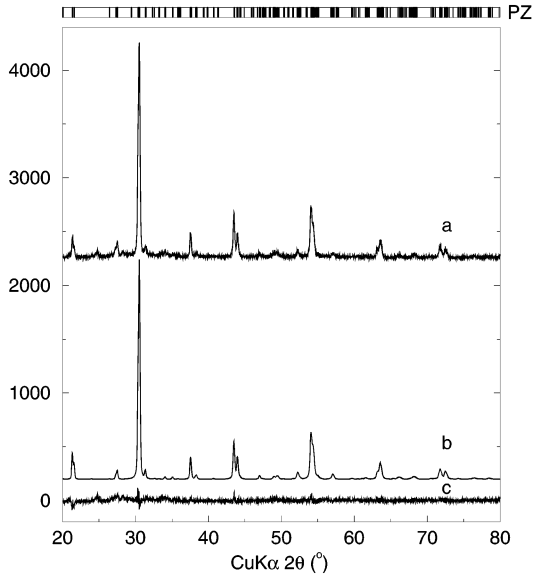

Figure 6. X-ray powder pattern of $PbZrO_3$ obtained from the previous composite by leaching away the K_2SO_4 component: (a) data, (b) Rietveld fit to the $PbZrO_3$, and (c) difference profile. Vertical lines at the top of the figure indicate expected peak positions for $PbZrO_3$ (PZ).

The SEM images of the $PbZrO_3/K_2SO_4$ monolith [Figure 7(a) and (b)] once again indicate small $PbZrO_3$ crystals dispersed in a matrix of larger K_2SO_4 crystals. This is particularly evident from the backscattered electron image in Figure 7(b). Leaching away of the large K_2SO_4 crystals results in the composite monolith breaking down to a powder. Thus, the present scheme did not succeed in obtaining a macroporous monolith as we had hoped. However, it does result in nearly pure, fine powder of $PbZrO_3$, the SEM image of which is displayed in Figure 7(c). It is shown that the particles are rather monodisperse, and <300 nm.

Discussion

The first question that needs to be addressed is the driving force for the metathetic exchange. At the simplest level, we propose that it is the high heat of formation of the alkali metal and alkaline earth sulfates that shifts the equilibrium of reactions 1 and 2 to the right. Table 2 lists heats of formation for ASO_4 (A = Ca, Sr, Ba) and $PbSO_4$.[31] It can be seen that the heat of formation of $PbSO_4$ is only about 60% that of the other sulfates. In reaction 2 it is possible that the formation of CO_2 provides an additional driving force. We did attempt, to no avail, metathetic reactions between $AZrO_3$ (A = Ca, Sr, Ba) and $PbCl_2$. In all the reactions, the large heats generated locally permit rapid product formation even at low external (furnace) temperatures.

A more sophisticated analysis is possible by considering the Gibbs free ($\Delta_f G^0$) energies of formation at 1000 K of the relevant species, data on most of which can found in the standard work of Barin and Knacke[32] and are listed in Table 3. This reference does not list data for $PbZrO_3$, however. Because this is the most important parameter for deciding whether the reactions should proceed, we have calculated the Gibbs free energy of formation for $PbZrO_3$ at 1000 K using three different sets of published data (which are not necessarily unrelated). First, we have used the value of $\Delta_f H^0$ (298 K) determined by Rane et al.[33] in conjunction with the values of S^0 (298 K) and $C_p(T)$ determined for $PbTiO_3$

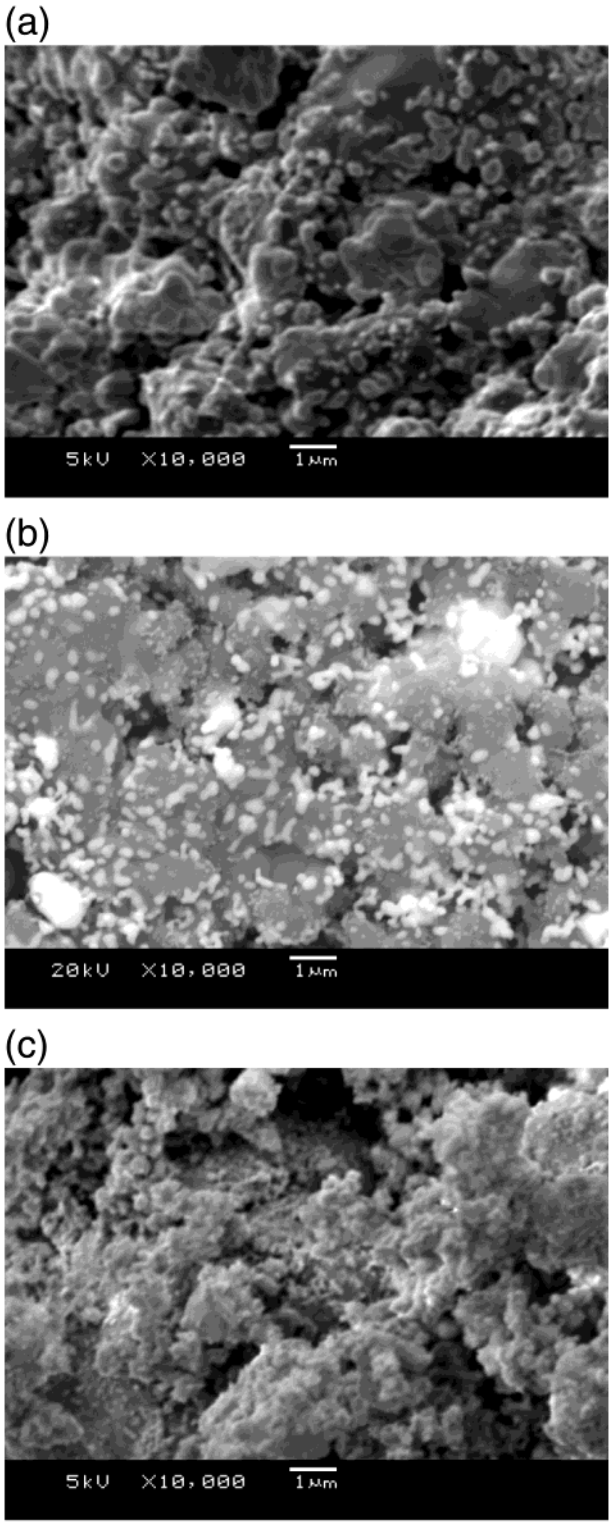

Figure 7. (a) SE and (b) backscattered electron SEM images of the $PbZrO_3/K_2SO_4$ composite; and (c) SE SEM image of the $PbZrO_3$ powder obtained by leaching away the K_2SO_4 component.

(31) Lide, D. R. (ed.). *CRC Handbook of Physics and Chemistry*, 80th ed.; CRC Press: Boca Raton, FL, 1999.

(32) Barin, I.; Knacke, O. *Thermochemical Properties of Inorganic Substances*; Springer-Verlag: Berlin, 1973; and Barin, I.; Knacke, O.; Kubachewski, O. *Thermochemical Properties of Inorganic Substances, Supplement*, Springer-Verlag, Berlin, 1977.

Table 2. Standard Enthalpies of Formations $\Delta_f H^0$ kJ mol^{-1} (ref 31)

$CaSO_4$	−1434.5
$SrSO_4$	−1453.1
$BaSO_4$	−1473.2
K_2SO_4	−1437.8
$PbSO_4$	−920.0

Table 3. Standard Gibbs Free Energies of Formation at 1000 K $\Delta_f G^0$ (1000 K) kJ mol^{-1} (ref 32)

$CaSO_4$	−1601.6	K_2CO_3	−1377.4
$SrSO_4$	−1624.7	CO_2	−630.37
$BaSO_4$	−1662.0	$CaZrO_3$	−1919.5
K_2SO_4	−1694.1	$SrZrO_3$	−1948.4
$PbSO_4$	−1122.0	$BaZrO_3$	−1942.8
ZrO_2	−1182.9	PbO	−310.51

Table 4. Miscellaneous Thermochemical Data Required to Calculate Gibbs Free Energy of Formation $\Delta_f G^0$ (1000 K) of $PbZrO_3$ at 1000 K

PbO	$\Delta_f H^0$ (1000 K)	−180.77 kJ mol^{-1}	ref. 32
ZrO_2	$\Delta_f H^0$ (1000 K)	−1050.0 kJ mol^{-1}	ref. 32
$PbZrO_3$	$\Delta_{f,oxides} H$ (973 K)	−2.63 kJ mol^{-1}	ref. 33
$PbZrO_3$	$\Delta_f H^0$ (298 K)	−1319.2 kJ mol^{-1}	ref. 33
$PbZrO_3$	$S°$ (298 K)	124.5 J mol^{-1} K	ref. 34
$PbZrO_3$	$C_p(T)$	$114.7 + 20.536 \times 10^{-3}$ T − 16.878×10^5 T^{-2} J mol^{-1} K	ref. 34

by Lencka and Riman.[34] These are listed in Table 4. We have then applied the following:

$$\Delta_f G^0(1000\ \text{K}) = [\Delta_f H^0(298\ \text{K}) + \int_{298}^{1000} C_p dT] - T\left[S^0(298\ \text{K}) + \int_{298}^{1000} \frac{C_p}{T} dT\right]$$

From this, we obtain for $PbZrO_3$, $\Delta_f G^0$ (1000 K) = −1517.7 kJ mol^{-1}.

In the second method, we have used the value of $\Delta_{f,oxides} H$ (973 K)[33] in conjunction with the values of $\Delta_f H^0$ (1000 K) for the oxides PbO and ZrO_2 as provided in reference 32 (Table 4). $\Delta_{f,oxides} H$ refers to the reaction $PbO(s) + ZrO_2(s) \rightarrow PbZrO_3(s)$. We have then used

$$\Delta_f G^0(1000\ \text{K}) \sim [\Delta_f H^0(973\ \text{K})] - T\left[S^0(298\ \text{K}) + \int_{298}^{1000} \frac{C_p}{T} dT\right]$$

From this we obtain for $PbZrO_3$, $\Delta_f G^0$ (1000 K) = −1538.8 kJ mol^{-1}.

The third method made use of a result presented by Lencka and Riman[34] for $PbZrO_3$: $\Delta_{f,oxides} G(T) = 13.160 - 21.43 \times 10^{-3}\ T$ kJ mol^{-1}, in conjunction with the $\Delta_f G^0$ (1000 K) values of PbO and ZrO_2.[32] From this, we obtain for $PbZrO_3$, $\Delta_f G^0$ (1000 K) = −1501.7 kJ mol^{-1}. The first two methods ignore the latent enthalpy of the paraelectric−antiferroelectric phase transition of $PbZrO_3$,[33] a value that is small compared to the spread in calculated $\Delta_f G^0$ (1000 K).

Table 5. Gibbs Free Energies of the Reactions at 1000 K

equation	Gibbs free energy $\Delta_r G$ (1000 K) kJ mol^{-1}
(1) with A = Ca	−61.8
(1) with A = Sr	−56.0
(1) with A = Ba	−98.9
(2)	−144.

Even if we consider the smallest of these values, $\Delta_f G^0$ (1000 K) =1501.7 kJ mol^{-1}, we calculate $\Delta_r G$ (1000 K) of the different reactions to be quite exothermic as seen from Table 5, varying from −61.8 kJ mol^{-1} to −144 kJ mol^{-1}. As suspected, the evolution of CO_2 makes the reaction corresponding to eq 2 the most exothermic.

The second point is the use of such metathesis for the production of composite materials and for small particles. During the metathetic exchange, one would expect complete dissolution (a term that we use to signify atomic-level mixing) followed by reprecipitation of the products. This means that small crystallites can be formed of one phase, whose growth is restricted by the other. Also, when one seeks ceramic/ceramic composites, the nature of the reprecipitation (somewhat akin to a spinodal decomposition) should permit intimate mixing of the two components in a manner that physically mixing the two phases would not achieve.

The third point is how we can change the reaction conditions so that the $PbZrO_3$ particles grow larger and bind to one another, so that a porous monolith of one phase, obtained upon leaching out the other, would retain its integrity. One possible way of achieving this is to add a flux that would help the $PbZrO_3$ crystallites to grow. Another possibility is to perform the metathesis under conditions of reactive hot-pressing.

We believe the work described here provides proof of concept that important perovskite materials such as $PbZrO_3$ can be prepared in various states of aggregation; as small particles, and as ceramic composites, by metathesis routes at relatively low temperatures. Using these approaches to prepare porous monoliths also looks promising. The approach could be easily extended to the synthesis of other related materials such as $PbTiO_3$.

Acknowledgment. This work has been supported by the Department of Science and Technology, India. It is a pleasure to thank Dr. U. Ramamurty for encouraging us to pursue the preparation of porous $PbZrO_3$, and Dr. S. Stemmer for help with the thermochemical calculations. P. E. D. Morgan and the anonymous reviewers are thanked for pointing out relevant references.

Supporting Information Available: Plots showing results of Rietveld refinement of the starting materials $AZrO_3$ (A = Ca, Sr, Ba) and SEM images of the composites $PbZrO_3/CaSO_4$ and $PbZrO_3/SrSO_4$ (PDF). This material is available free of charge via the Internet at http://pubs.acs.org.

CM021065Z

(33) Rane, M. V.; Navrotsky, A.; Rossetti, G. A. *J. Solid State Chem.* **2001**, *161*, 402.
(34) Lencka, M. M.; Riman, R. E. *Thermochim. Acta* **1995**, *256*, 193.